Protein Engineering, Design & Selection vol. 26 no. 2 pp. 133–142, 2013
Published online November 15, 2012 doi:10.1093/protein/gzs094

Engineering a soluble high-affinity receptor domain that neutralizes staphylococcal enterotoxin C in rabbit models of disease

D.M.Mattis[1], A.R.Spaulding[2,4], O.N.Chuang-Smith[2], E.J.Sundberg[3,5], P.M.Schlievert[2,4] and D.M.Kranz[1,6]

[1]Department of Biochemistry, University of Illinois, Urbana, IL 61801, USA, [2]Department of Microbiology, University of Minnesota Medical School, Minneapolis, MN 55455, USA, [3]Boston Biomedical Research Institute, Watertown, MA 02472, USA, [4]Present address: Department of Microbiology, University of Iowa, Iowa City, IA 52242, USA and [5]Present address: Institute of Human Virology, Department of Medicine, University of Maryland School of Medicine, Baltimore, MD 21201, USA

[6]To whom correspondence should be addressed:
E-mail: d-kranz@illinois.edu

Received August 31, 2012; revised August 31, 2012; accepted October 17, 2012

Edited by James Marks

Superantigens (SAgs) are a class of immunostimulatory exotoxins that activate large numbers of T cells, leading to overproduction of cytokines and subsequent inflammatory reactions and systemic toxicity. Staphylococcal enterotoxin C (SEC), a SAg secreted by *Staphylococcus aureus*, has been implicated in various illnesses including non-menstrual toxic shock syndrome (TSS) and necrotizing pneumonia. SEC has been shown to cause TSS illness in rabbits and the toxin contributes to lethality associated with methicillin-resistant *S.aureus* (MRSA) in a rabbit model of pneumonia. With the goal of reducing morbidity and mortality associated with SEC, a high-affinity variant of the extracellular variable domain of the T-cell receptor beta-chain for SEC (∼14 kDa) was generated by directed evolution using yeast display. This protein was characterized biochemically and shown to cross-react with the homologous (65% identical) SAg staphylococcal enterotoxin B (SEB). The soluble, high-affinity T-cell receptor protein neutralized SEC and SEB *in vitro* and also significantly reduced the bacterial burden of an SEC-positive strain of MRSA (USA400 MW2) in an infective endocarditis model. The neutralizing agent also prevented lethality due to MW2 in a necrotizing pneumonia rabbit model. These studies characterize a soluble high-affinity neutralizing agent against SEC, which is cross-reactive with SEB, and that has potential to be used intravenously with antibiotics to manage staphylococcal diseases that involve these SAgs.

Keywords: directed evolution/staphylococcal enterotoxin B (SEB)/staphylococcal enterotoxin C (SEC)/yeast display

Introduction

The Gram-positive bacterium *Staphylococcus aureus* is responsible for a wide spectrum of diseases, with infections that can target skin and mucous membranes, heart, lungs, bones and blood (Lowy, 1998; Mertz *et al.*, 2007). Among the major factors associated with severity of *S.aureus* illnesses is a class of secreted exotoxins called superantigens (SAgs). These exotoxins are a group of relatively small (19–30 kDa) proteins variably produced by *S.aureus* strains (Fraser and Proft, 2008). The term 'superantigen' was given to these toxins because their major systemic toxicity depended on the abilities of the toxins to stimulate uncharacteristically large proportions of T cells, causing massive production of pro-inflammatory molecules, including tumor necrosis factor-α (TNF-α), interleukin (IL)-1, IL-2 and interferon-γ (IFN-γ) (Marrack and Kappler, 1990; Li *et al.*, 1999).

The mechanism of superantigenicity is now understood at both biochemical and structural levels. The activity requires SAg binding to the Vβ region of the heterodimeric T-cell receptor (Vβ) and simultaneously to class II products of the major histocompatibility complex (MHC II). While conventional peptide/MHC complexes stimulate relatively small numbers of T cells in the body (usually $<0.01\%$), SAgs may stimulate up to 30% of T cells (Marrack and Kappler, 1990; Papageorgiou and Acharya, 1997; Li *et al.*, 1999). The major systemic effects of SAgs that result from these interactions are fever, hypotension and skin rash production (Fraser and Proft, 2008).

The potency in hyperactivation of the immune system makes staphylococcal SAgs capable of incapacitation and lethality, and appears responsible for their involvement in multiple illnesses. While perhaps best known as the direct cause of toxic shock syndrome (TSS), in recent years SAgs have been increasingly implicated in several other illnesses, including airway diseases, necrotizing pneumonia and purpura fulminans (Luppi *et al.*, 1998; Bachert *et al.*, 2007; Strandberg *et al.*, 2010). *Staphylococcus aureus* is also a leading cause of infective endocarditis (Sacar *et al.*, 2010), an illness that is characterized by colonization of damaged heart valves by *S.aureus* strains, leading to the production of cauliflower-appearing vegetations composed of bacterial colonies and host cells. We have shown previously that the SAg TSS toxin-1 (TSST-1), under regulation of the SrrAB two-component regulatory system, may be one of the virulence factors contributing to development of infective endocarditis (Pragman *et al.*, 2004). It was hypothesized that the infective endocarditis hallmark of vegetations, consisting of lesions with biofilm-appearing colonies of *S.aureus*, may be associated with SAg-mediated, immune system dysregulation. Supporting a possible role of SAgs, a recent analysis of methicillin-susceptible *S.aureus* (MSSA) endocarditis showed that the TSST-1 gene was among only a few genes that were significantly associated with isolates derived from endocarditis patients, in distinct contrast to isolates from soft tissue infections (Nienaber *et al.*, 2011). In the study, over 90% of the MSSA strains that caused endocarditis in patients from North America, Europe and Australia expressed the TSST-1 gene.

Methicillin-resistant *S.aureus* (MRSA)-producing SAgs pose added problems in management of staphylococcal illnesses, due to their increased difficulty in treatment associated with antibiotic resistance and SAg toxicity (Resch *et al.*, 2009). Our recent studies with a rabbit model showed that SAgs play an important role in the lethality associated with pulmonary infections caused by community-associated (CA)-MRSA (Strandberg *et al.*, 2010), including the highly-studied CA-MRSA USA400 strain MW2 that secretes SEC (Fey *et al.*, 2003).

In the present study, based on success with the high-affinity-engineered SEB antagonist Vβ G5-8 (Buonpane *et al.*, 2007), we sought to develop a high-affinity Vβ against SEC that could be used *in vivo* as a potential therapeutic. Guided by the structure of SEC in complex with several variants of the Vβ8, and a first-generation engineering effort (Kieke *et al.*, 2001; Cho *et al.*, 2005), we took a rational design approach, combined with directed evolution using yeast display (Boder and Wittrup, 2000) to improve the affinity of the Vβ8 for SEC. Unexpectedly, based on previous studies with SEB-reactive Vβ regions (Wang *et al.*, 2010), our highest affinity Vβ ($K_D = 2$ nM for SEC) called L3 was also able to cross-react with high affinity for the SAg SEB ($K_D = 4$ nM for SEB), which shares 65% sequence identity with SEC (Bohach *et al.*, 1990; McCormick *et al.*, 2001). The L3 Vβ neutralized both SEC and SEB in an *in vitro* T-cell assay. We also tested the *in vivo* efficacy of L3 in four different rabbit models of SEC toxicity. L3 prevented the lethality associated with direct exposure to purified recombinant SEC, and it was effective in two different rabbit models with the SEC-positive MRSA strain MW2 (USA400), including infective endocarditis and necrotizing pneumonia models.

Materials and methods

Yeast display libraries and cloning

The gene encoding the mouse Vβ8 mutant called L2CM (Kieke *et al.*, 2001) was cloned into yeast display vector pCT302, which contains an N-terminal haemagluttinin (HA) tag and a C-terminal Myc (c-myc) tag (Fig. 1A) (Boder and Wittrup, 2000). Libraries of mutants in L2CM were constructed in the CDR2 (residues 52–56) and HV4 (residues 70–74) regions by site-directed mutagenesis using overlapping degenerate primers. The mutant called L3 was cloned by introducing the mutations of clone HV7 into the mutant CD6 using QuikChange as described by the manufacturer (Stratagene, La Jolla, CA, USA).

Selection and analysis of Vβ mutants by flow cytometry

Expression of Aga2p fusions were induced by growth of yeast cells in medium containing galactose at 20°C for 32–48 h. After induction, yeast-displayed Vβ proteins were selected by fluorescence-activated cell sorting (FACS) or analyzed by flow cytometry. Yeast cell libraries were selected by using equilibrium or off-rate-based methodologies. For equilibrium sorting, the yeast library was incubated with various concentrations of biotin-SEC3 (Toxin Technology, Sarasota, FL, USA) in phosphate-buffered saline (PBS) for 1 h on ice. Cells were washed with 0.5 ml PBS–0.05% bovine serum albumin (PBS–BSA) and then incubated with streptavidin–phycoerythrin (SA–PE) (BD Biosciences) at a 1 : 1000 dilution. Libraries were selected using FACS analysis (MoFlo; Cytomation). Off-rate selection was performed by incubation of yeast libraries with biotin-SEC3 under equilibrium conditions, followed by washing, incubation with non-biotinylated SEC3 in 10-fold molar excess at 25°C for various times, followed by SA–PE staining.

Yeast cells isolated by FACS were either expanded by culturing for subsequent rounds of selection, or plated on selective medium to isolate yeast clones. Individual clones were analyzed for equilibrium and off-rate binding to biotin-SAg. Equilibrium binding was performed as described above for sorting, except that either biotin-SEC3 or biotin-SEB was used. Off-rate analysis was performed as described above for sorting, except that the second incubation with unlabeled SEC3 was performed at 37°C rather than at 25°C. Samples at various time points were analyzed and percent-bound biotin-SEC (mean fluorescence units (MFUs) of samples at specific time point/MFUs at time point zero × 100) was plotted against time. C-myc and HA tag expression were used to estimate surface expression of clones. Cells were analyzed on a Coulter Epics XL flow cytometer or a BD Accuri C6 flow cytometer.

Cloning, expression and purification of soluble Vβ proteins

Vβ mutant L3 was subcloned as an NheI–BglII fragment into the pET28 expression vector (Novagen) for expression in bacteria. The Vβ proteins L3, L2CM, G5-8 and mTCR15 were expressed in BL21 (DE3) *Escherichia coli*, refolded *in vitro* from inclusion bodies, and purified with Ni agarose resin (Qiagen), followed by gel filtration high-performance liquid chromatography (BioCad Sprint) using a size exclusion Superdex 200 column (Pharmacia) in PBS (pH 7.4) as described previously (Buonpane *et al.*, 2007). Protein preparations were examined by sodium dodecyl sulfate polyacrylamide gel electrophoresis (SDS-PAGE) and mass spectrometry. For mass spectrometry analysis, purified protein was equilibrated with ammonium acetate buffer and then analyzed at the UIUC Mass Spectrometry Laboratory by Electrospray Ionization on a Quattro II mass spectrometer using Masslynx software.

Binding of soluble Vβ to SAg

Binding of soluble Vβ to biotinylated-SAg was examined by enzyme-linked immunosorbent assay (ELISA) and surface plasmon resonance (SPR). For the ELISAs, Vβ protein was coated on ELISA wells (5 μg/ml), followed by addition of various concentrations of biotin-SEC3 or biotin-SEB, followed by streptavidin-conjugated horseradish peroxidase (BD Biosciences), and finally substrate to yield a colorimetric read-out at an absorbance of 450 nM wavelength. The affinities and kinetic parameters of Vβ : SEC3 and Vβ : SEB interactions were determined by SPR analysis using a BIAcore 3000 instrument as described previously (Kieke *et al.*, 2001; Buonpane *et al.*, 2007).

T-cell assays

T-cell hybridoma line m6-16 cells (5×10^5 cells/ml) that expresses a TCR with the mouse Vβ8.2 region (Holler and Kranz, 2003) were stimulated with 35 nM SAg (SEC3 or SEB) in the presence of MHC class II-positive B cell line LG-2 cells (10^5 cells/ml). Soluble Vβ proteins (L3, L2CM, G5-8 or negative control mTCR15) were added at various

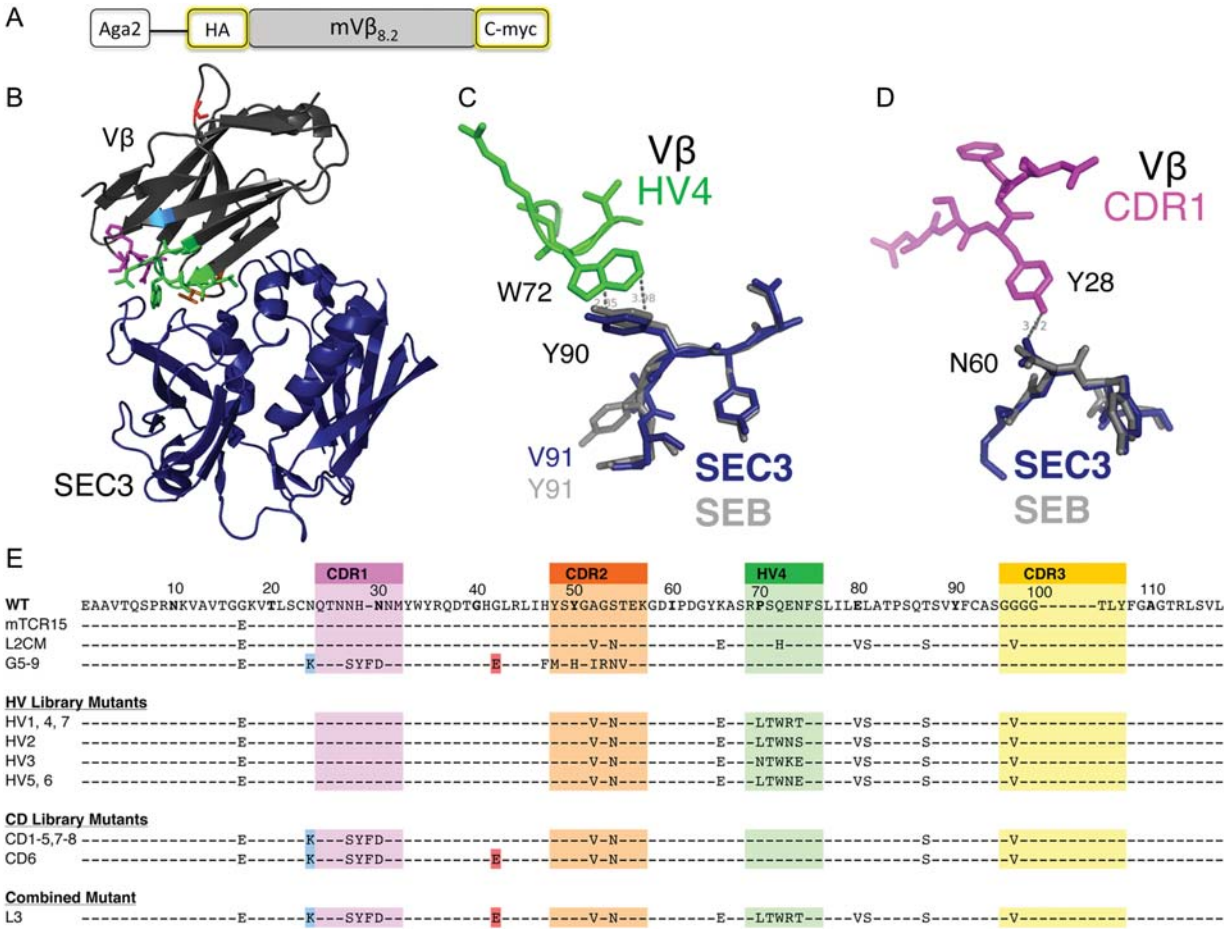

Fig. 1. Vβ8 mutants against SEC3 isolated by yeast display. (**A**) Vβ8.2 gene (L2CM) was fused to Aga2 for expression on the surface of yeast cells. The Vβ gene was flanked by HA and C-myc epitopes. (**B**) Crystal structure of the Vβ8 mutant L2CM (dark gray) in complex with SEC3 (dark blue). Mutations A52V and S54N in the CDR2 region were selected previously by random PCR mutagenesis for improved affinity of L2CM to SEC (Kieke *et al*., 2001) and are shown in orange. Residues mutated to generate L3 are in CDR1 (residues 28–30, magenta), in HV4 (residues 70–74, green) and individual residues Gly24 (marine blue) and Gly42 (red). Figure based on PDB file 2AQ3. (**C**) Model of the L2CM structure with L3 substituted mutations in the HV4 region, showing aromatic base stacking between L3 : W72 and overlay of SEB/SEC3 Y90 that may contribute to improved affinity of L3 for both SEB and SEC. Model based on PDB files 2AQ3 and 3R8B. (**D**) Model of CDR1 loop of G5-8 in complex with SEB/SEC3 overlay, showing the likely interaction between L3 : Y28 and SEC/SEB : N60, contributing to improved affinity by the CDR1 mutations (Bonsor *et al*., 2011). Model based on PDB files 2AQ3 and 3R8B. (**E**) Sequences of Vβ8 mutants isolated by yeast display. Unique sequences of clones selected from the HV and CD libraries are listed. The two highest affinity mutants identified from yeast display library selection were HV7 and CD6. HV7 contains mutations in the HV4 region (green), and CD6 contains mutations in the CDR1 region (magenta). Combining the mutations in HV7 and CD6 generated the highest affinity mutant, L3. mTCR15 refers to a single-site mutant that had improved display on yeast compared with the wild-type Vβ8, but retains the wild-type residues that contact SEC3. G5-9 refers to a high-affinity Vβ previously developed in our laboratory against SEB (Buonpane *et al*., 2007).

concentrations and incubated at 37°C for 20–24 h. Cells were centrifuged, and supernatants were collected. IL-2 levels in supernatants were measured by ELISA.

Bacterial strain

CA-MRSA USA400 strain MW2 was originally obtained in the Upper Midwest from a young patient who succumbed to necrotizing pneumonia. The strain of low passage is maintained in the lyophilized state in the Schlievert laboratory. Genome-sequencing studies of MW2 indicated that the strain has the potential to produce the SAgs SEC, SEA and the SE-like SAgs H, K, L, Q and X (Derzelle *et al*., 2009). Our studies of MW2 and other *S.aureus* strains reported findings show that SEC is expressed at orders of magnitude higher levels than the other genes in certain strains and thus is likely to be more involved in the diseases caused by SAgs. For example, in the MW2 strain, SAg levels in culture supernatants were determined as follows: SEC, 77 000 ng/ml; SEA, 0.15 ng/ml; SE-like H, 0.075 ng/ml; SE-like K, 0.075 ng/ml; SE-like L, 0.075 ng/ml; SE-like Q, 30 ng/ml and SE-like X, 0.1 ng/ml. These SAg levels were determined by quantitative Western immunoblots, which utilizes purified toxins tested comparably as standards. This method of toxin quantification has been reported previously (Schlievert *et al*., 2007).

Animal studies

All animal experiments were performed according to protocols approved by the Institutional Animal Care and Use Committee (IACUC) of the University of Minnesota.

Endotoxin enhancement model

New Zealand White (NZW) rabbits (~2 kg each) were injected intravenously (i.v.) with 5 μg/kg of the SAg SEC3

in PBS either alone or in combination with 100 μg/kg soluble Vβ L3 in PBS, followed 4 h later with i.v. injections of 0.15 μg/kg/ml endotoxin (*Salmonella typhimurium*). SAgs have been shown to amplify the effects of endotoxin through synergistic release of TNF-α (Schlievert, 1982; Dinges and Schlievert, 2001). Temperatures were monitored for 4 h after injection. The rabbits were monitored for up to 48 h for signs of fever, diarrhea and death. *P* value determined by Fisher's exact test ($n = 9$ per group).

Miniosmotic pump model

In this model, Dutch-belted rabbits receive continuously released SEC3 from subcutaneously implanted miniosmotic pumps (Alza, Palo Alto, CA, USA) (Parsonnet *et al.*, 1987). Young adult rabbits (~1–2 kg) were anesthetized with ketamine and xylazine, and incisions were made on the left flanks. A subcutaneous pocket was made in each rabbit large enough to accommodate the miniosmotic pump. The miniosmotic pumps are loaded with 200 μg SAg and implanted in the pocket. The rabbits were sutured, allowed to wake, returned to their cages and monitored for temperature on Day 2, and TSS symptoms and death over 8 days. In this model, the maximum fever occurs on Day 2. Soluble 100 μg Vβ or the control PBS was administered i.v. once daily for 7 days. *P* value determined by two-tailed unpaired *t*-test ($n = 3$ per group). The error bars represent standard error of mean.

MW2 necrotizing pneumonia

NZW rabbits (~2 kg each) were anesthetized with ketamine and xylazine and incisions were made through the neck fur and then in the trachea. The animal was placed on its right side to insert a catheter through the trachea into the right bronchi. Approximately 1.8×10^9 bacteria were injected, the trachea sealed and the incision sutured. The animal was allowed to wake and was then returned to its cage and monitored. This model of necrotizing pneumonia has been described previously (Strandberg *et al.*, 2010). The experiment used SEC-secreting USA400 CA-MRSA strain (MW2). Rabbits were administered an i.v. bolus of either the control PBS (pH 7.4) or 500 μg Vβ L3 once daily. Rabbit temperatures and survival were monitored daily over 4 days. *P* value determined by log-rank (Mantel–Cox) test ($n = 4$ per group).

MW2 endocarditis

NZW rabbits were anesthetized and underwent surgery to insert catheters through the left carotid arteries to the aortic valves, where the catheters remained for 2 h (Schlievert *et al.*, 1998; Pragman *et al.*, 2004). The experiments consisted of two groups of rabbits ($n = 4$ per group). Either the control PBS (pH 7.4) or 100 μg of Vβ L3 was injected i.v. through the marginal ear vein of the NZW rabbits (~2 kg each), followed by the SEC-secreting microbe CA-MRSA USA400 strain MW2 in the range of 9×10^7–1×10^8 bacteria. The rabbits were administered either control PBS or 100 μg of Vβ L3 twice a day for up to 4 days. The rabbits were examined daily for survival and upon premature death, or on Day 4 for vegetations.

Results

Yeast display and engineering of high-affinity anti-SEC Vβ mutants

To engineer soluble, high-affinity SEC antagonists, we used a mouse Vβ8 gene cloned as an Aga-2 fusion in the yeast display vector pCT302 (Fig. 1A) (Boder and Wittrup, 2000). Previously in our laboratory, random mutagenesis was used to affinity-mature the wild-type Vβ8 against SEC, resulting in the mutant called L2CM (Kieke *et al.*, 2001). However, our more recent studies have shown that site-directed mutagenesis approaches could yield significantly higher affinities (e.g. in the 50–200 pM range) for Vβ mutants against the SAg SEB, providing more potent *in vitro* and *in vivo* neutralizing agents (Buonpane *et al.*, 2007). To accomplish this with the SEC system, L2CM was used as the starting template for a directed evolution strategy with specific site-directed libraries of mutants.

Based on alanine scanning mutagenesis (Churchill *et al.*, 2000) and crystal structures (Cho *et al.*, 2005), Vβ residues at the interface of the Vβ : SEC complex were mutated to generate two libraries, one in hypervariable region 4 (hereafter termed HV library) and one in complementarity determining region 2 (hereafter referred to as CD library) (Fig. 1B). Detailed description of generating, sorting and identifying clones from each of the two libraries are provided in Supplementary Results. The two yeast display libraries yielded various clones with improved binding to SEC3, compared with L2CM (Fig. 2A and B). The clones derived from the HV library also showed improved off-rates, as evidenced by a greater fraction of bound biotin-SEC3 after incubation with excess unlabeled SEC3 for 10 min (Fig. 2C). A single CD clone, CD6, also showed a slight improvement in off-rate.

Among the HV mutants, there were four unique sequences (Fig. 1E), all containing the same mutations at two of the five positions in the HV4 region: S71T and H72W, suggesting that these mutations were important for improved affinity. There also appeared to be preferences for leucine at position 70 (3/4), asparagine at position 73 (2/4) and glutamic acid at position 74 (2/4) (Fig. 1E and Supplementary Fig. S2A). Based on modeling of the crystal structure L2CM in complex with SEC3, we believe that mutation Trp72 in L3 could interact with Tyr90 in SEC3 (Fig. 1C).

The sequences of eight CD clones showed that, unexpectedly, there were no mutations in the CDR2 region but there were mutations in or near the CDR1 region, at positions 24 and 28–30. One clone (CD6) contained an additional mutation at position 42. The origin of these mutations is almost certainly due to the original pCT302 vector which contained the high-affinity Vβ mutant called G5-9, developed against SEB, and was used to clone the polymerase chain reaction (PCR) products of the HV4 and CDR2 libraries (Fig. 1E) (Buonpane *et al.*, 2007). Thus, during the homologous recombination step involving yeast transformation of the libraries, there was likely a low frequency of recombination between undigested pCT302/G5-9 and the PCR-amplified libraries of L2CM. The prevalence of the G5-9/L2CM chimera in the SEC-selected library suggests that other CDR2 mutations in the library were not preferred above the A52V and S54N mutations of L2CM, and that the CDR1 of G5-9 provided some improvement above L2CM in SEC binding (as it did with

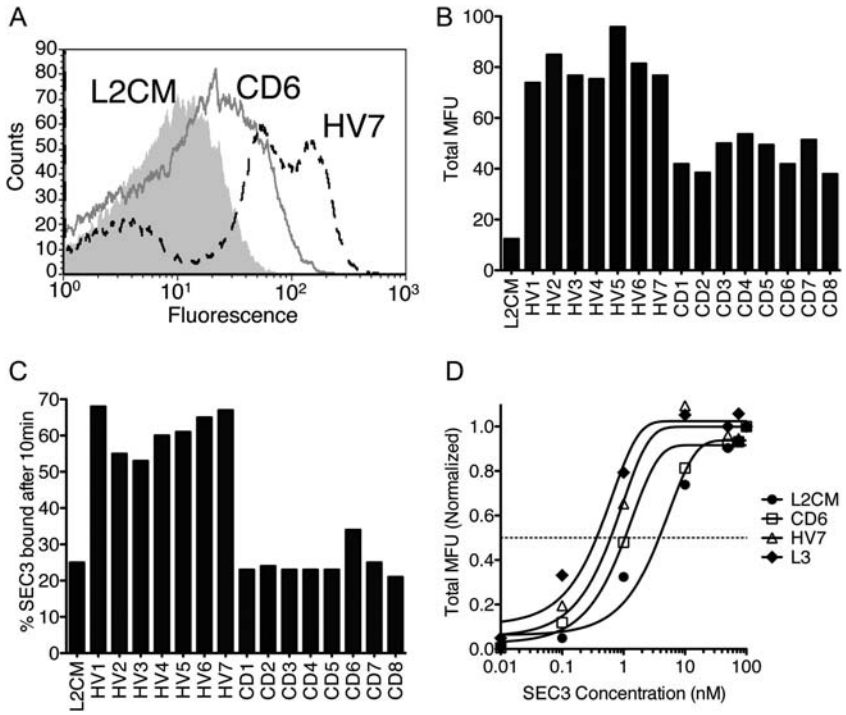

Fig. 2. Yeast displayed clones analyzed for SEC3 binding by flow cytometry. (**A**) Flow cytometry histograms of L2CM, HV7 and CD6 after staining with 0.1 nM biotin-SEC3, followed by SA–PE. (**B**) MFU of various Vβ8 mutants stained with 0.1 nM biotin-SEC3 followed by SA–PE. (**C**) %SEC3 remaining bound to various Vβ8 mutants following incubation with 0.5 nM biotinylated-SEC3, 10 min after addition of 10-fold molar excess of unlabeled SEC3. (**D**) L2CM, the two highest-affinity clones selected from each library (CD6 and HV7), and the combined mutant L3 were titrated with 0.01 nM to 100 nM SEC3, followed by SA–PE. The normalized MFUs were obtained by flow cytometry and plotted against SEC3 concentration to generate the binding curves.

SEB). In fact, the recent crystal structure of a related SEB-binding mutant called G5-8 shows that the Tyr28 mutation of CDR1 contacts residue Asn60 that is conserved between SEB and SEC (Fig. 1D) (Bonsor *et al.*, 2011).

As clones HV7 and CD6 had improved binding, and we have shown previously that such mutations can yield synergistic binding when combined (Kieke *et al.*, 2001; Moza *et al.*, 2006), the HV7 and CD6 mutations were introduced into a single mutant called L3 (Fig. 1E). Yeast display titrations with SEC showed that mutant L3 had an affinity that was improved slightly above that of both HV7 and CD6 (Fig. 2D), and thus L3 was used for further studies with soluble Vβ protein and neutralization of SEC.

Analysis of L3 Vβ regions for SEB binding

Since L3 shared the same CDR1 mutations as the SEB affinity matured mutant G5-9, and the SAgs SEB and SEC3 share the common residue Tyr90 that we believe interacts with L3 Trp72, we decided to test yeast display binding of L3 to SEB. We found that yeast displayed L3 bound to 10 nM biotin-SEB (Fig. 3). In contrast, the Vβ engineered for high-affinity binding to SEB, called G5-8, did not bind SEC3, although as expected it bound to SEB (Buonpane *et al.*, 2007).

The mutations in L3 originated from one of three sources: CDR2 mutations in the template L2CM, HV4 mutations from mutant HV7 or CDR1 mutations from mutant CD6 (Fig. 1E). To determine which mutations in L3 were responsible for the cross-reactivity with SEB, yeast displayed Vβ regions CD6, HV7 and L2CM were also analyzed with

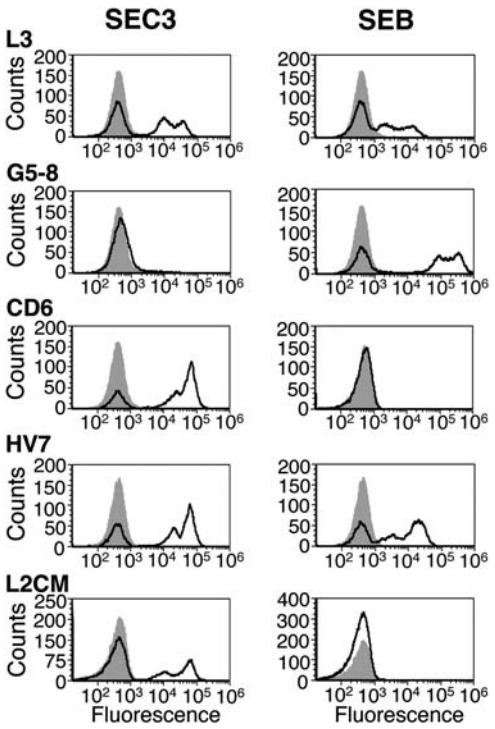

Fig. 3. Yeast display high-affinity Vβ mutants stained with 10 nM SEC3 and SEB. Vβ mutants L3, G5-8, CD6, HV7 and L2CM were stained with 10 nM biotin-SEC3 (left column) or 10 nM biotin-SEB (right column), followed by SA–PE. Mutants L3 and HV7 bound both SAgs. CD6 and L2CM bound only 10 nM SEC3. G5-8 bound only 10 nM SEB. Gray peak indicates background fluorescence. Black line indicates fluorescence of Vβ mutant.

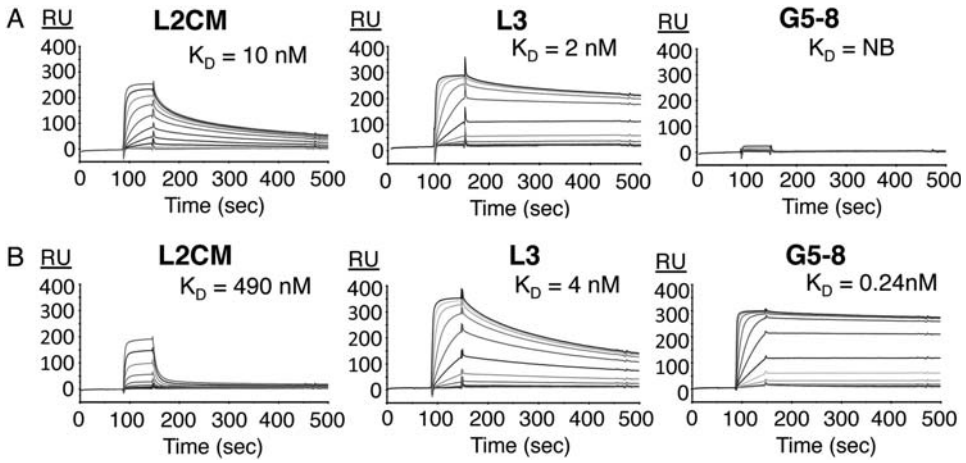

Fig. 4. Binding (SPR) of soluble Vβ8 proteins. (**A**) SPR traces of serial 2-fold dilutions (800 nM stocks) of affinity-matured Vβ8 mutants L2CM, L3 and G5-8 injected at a flow rate of 25 μl/min over immobilized (A) SEC3 or (**B**) SEB, as previously described (Buonpane *et al*., 2007). RU, response units. Binding affinity (K_D) are shown, NB, no binding.

10 nM biotin-SEB and 10 nM biotin-SEC3 (Fig. 3). Mutants L3, CD6, HV7 and L2CM that were selected for improved SEC3 binding, all bound 10 nM SEC3 (Fig. 3, left-hand column), as was originally observed in the process of yeast display selections. Binding to 10 nM SEB was observed for L3, G5-8 and HV7 (Fig. 3, right-hand column). Neither L2CM nor CD6 showed detectable binding to 10 nM SEB. The detectable binding of SEB by HV7 indicates that the HV4 mutations, including the tryptophan at position 72, were important in binding to SEB. As indicated, a possible interaction might occur between Trp72 of the L3 HV4 region and Tyr90 of SEC, and this residue (Tyr90) is also present in SEB (Fig. 1C).

Expression, purification and SAg binding analyses of soluble Vβ proteins

To produce soluble protein for neutralization studies, the Vβ proteins, including L3, were expressed and refolded from inclusion bodies in *E.coli*. After refolding and nickel resin affinity purification, the L3 protein eluted as a monomer on gel filtration chromatography and exhibited the expected sizes by SDS-PAGE and mass spectrometry (calculated size based on amino acid sequence, 14 566 Da; size observed on mass spectrometry, 14 563 Da) (data not shown). The protein yield averaged 2 mg/l of inclusion bodies.

L3, L2CM and G5-8 proteins were examined using SPR to measure the affinity and kinetics of their interactions with SEB and SEC3 (Fig. 4 and Table I). The affinity constants (K_D values) for SEC (Fig. 4A) were 10 nM (L2CM) and 2 nM (L3), while G5-8 showed no detectable binding, consistent with the flow cytometry results. Compared with L2CM, L3 also exhibited an ~7-fold improvement in off-rate, suggesting that HV4 and CDR1 mutations increase the stability of the complex with SEC3. The half-life ($t_{1/2}$) of the complex at 25°C was thus predicted to be ~20 min.

Consistent with flow cytometry results, the affinity of L3 for SEB ($K_D = 4$ nM) was shown to be considerably higher, by about 100-fold, than the affinity of L2CM for SEB ($K_D =$ 490 nM) (Fig. 4B). Thus, it is possible to generate a cross-reactive, high-affinity Vβ, by manipulating different regions of the interface, focusing in principle on residues that are shared between SEC and SEB.

Table I. SPR results of high-affinity Vβs

Vβ	SAg SEC3			SAg SEB		
	k_a (M^{-1} s^{-1})	k^d (s^{-1})	K_D (nM)	k_a (M^{-1} s^{-1})	k^d (s^{-1})	K_D (nM)
L2CM	3.96×10^5	3.94×10^{-3}	10	ND[a]	ND	490
L3	2.68×10^5	5.75×10^{-4}	2	6.7×10^5	2.57×10^{-3}	4
G5-8	NB[b]	NB	ND	5.75×10^5	1.4×10^{-4}	0.24

[a]ND, not determined.
[b]NB, no binding.

In vitro *neutralization of SAg-mediated activation of T cells*

To analyze the SEC and SEB neutralization ability of mutant L3, we monitored the release of IL-2 by a T-cell line that expresses the Vβ8 region. In this assay IL-2 is secreted when the Vβ8-positive T cell line is incubated with SAg (35 nM) and a human class II MHC-positive B cell line called LG-2. The soluble high-affinity Vβ proteins L3, G5-8, L2CM and mTCR15 (a wild-type Vβ8 proteins that has a single mutation allowing expression in soluble form; Kieke *et al*., 2001) were added at various concentrations, and after ~24 h the supernatants were assayed for IL-2 levels using a capture ELISA. The wild-type Vβ (mTCR15), which has micromolar affinity for both SEC3 and SEB, was ineffective at neutralizing either SAg (Fig. 5). In contrast, L2CM was able to completely neutralize SEC3 activity with an IC_{50} of 400 nM, and L3 was able to completely neutralize SEC3 activity with an IC_{50} of 40 nM (Fig. 5A). Thus, L3 exhibited ~10-fold improved inhibitory properties, consistent with its 7-fold enhanced lifetime of dissociation compared with L2CM. The Vβ G5-8 that was developed against SEB was unable to neutralize SEC (Fig. 5A), but was effective at neutralizing SEB activity (Fig. 5B). In contrast, L3 was able to neutralize both SEB activity (Fig. 5B) and SEC activity, as anticipated from the results of binding studies.

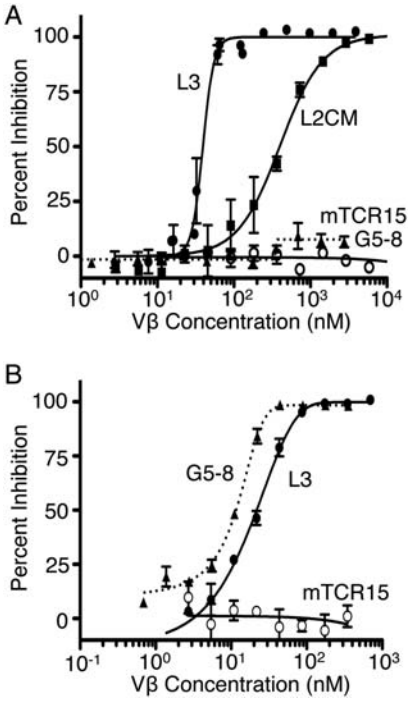

Fig. 5. *In vitro* inhibition of SEC3- and SEB-mediated T cell activity by soluble Vβ proteins. T cell cytokine (IL-2) release assay showing inhibitory activity of soluble, high-affinity Vβ mutants L3 (filled circles), L2CM (filled squares), G5-8 (filled triangle, dotted line) and the wild-type Vβ mTCR15 (open circles) against (**A**) SEC3 and (**B**) SEB. Mutants were added at the indicated concentrations to wells containing the Vβ8-positive T cell line m6-16, SAg and the human class II-positive B cell line LG-2. The error bars represent SEM ($n = 2$ per group).

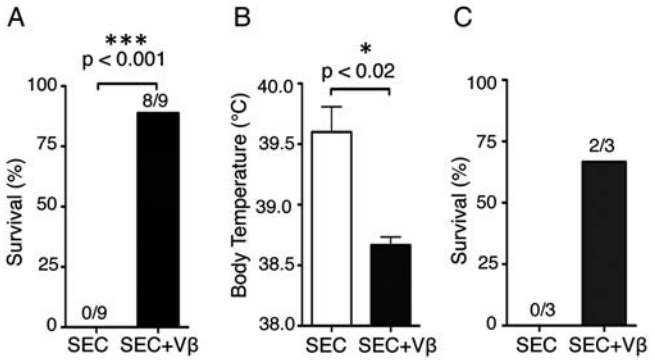

Fig. 6. *In vivo* models testing Vβ L3 neutralization of SEC3. (**A**) LPS enhancement model. Rabbits were injected i.v. with either the SAg SEC alone or in combination with the Vβ L3, followed 4 h later with LPS. Zero of nine rabbits survived when injected with SEC alone. L3 is able to neutralize the toxin yielding survival of 8/9 rabbits. *P* value determined by Fisher's exact test ($n = 9$ per group). (**B**) and (**C**) Miniosmotic pump model. Rabbits were surgically implanted with a pump that releases either the SAg SEC alone or in combination with the Vβ L3. Second day body temperatures were significantly increased and 0/3 rabbits survived when injected with SEC alone versus survival of 2/3 rabbits and reduced body temperatures when treated with Vβ L3. (**B**) *P* value determined by two-tailed unpaired *t* test ($n = 3$ per group). The error bars represent SEM.

Neutralization of SEC by the soluble Vβ L3 in an endotoxin enhancement rabbit model

To determine whether Vβ L3 could neutralize SEC *in vivo*, we used SEC in an endotoxin enhancement rabbit model, which lowers the lethal doses of both SEC and endotoxin by orders of magnitude (Schlievert, 1982; Dinges and Schlievert, 2001). NZW rabbits were injected with 5 μg/kg SEC3 followed by either PBS or the soluble Vβ L3 at 100 μg/kg. After 4 h, each rabbit was injected i.v. with 0.15 μg/kg of endotoxin lipopolysaccharide (LPS), which is 100 times the half-maximal lethal dose (LD_{50}) in rabbits pretreated with 5 μg/kg SEC3 (the LD_{50} of LPS alone is 500 μg/kg). After 48 h, none of the nine rabbits that received PBS survived, while eight of the nine rabbits that received the soluble Vβ L3 survived (Fig. 6A). The ability of the L3 protein to prevent death in this model was highly significant ($P < 0.001$).

Neutralization of SEC by the soluble Vβ L3 in a miniosmotic pump rabbit model

In a bacterial infection, SAg is thought to be produced continuously by the bacteria. To simulate this, a miniosmotic pump releases ~200 μg of SEC3 over an 8-day period. In this model, either PBS or 100 μg of Vβ L3 was administered i.v. daily ($n = 3$ per group). The second-day body temperatures of the rabbits that received the control PBS averaged 39.6°C, which was significantly greater than the rabbits that received the Vβ L3, which were 38.7°C (Fig. 6B). Although these values differ only by a degree, the difference is significant, with a *P* value < 0.05. Two of the three rabbits that received the Vβ L3 survived, while none of the three rabbits that received the control PBS survived (Fig. 6C).

Neutralization of SEC secreted by MW2 in a necrotizing pneumonia rabbit model

To examine the ability of Vβ L3 to neutralize SEC secreted from bacteria, we used a necrotizing pneumonia rabbit model. This model is appropriate because SEC is implicated as playing a role in the development of necrotizing pneumonia (Strandberg *et al*., 2010). NZW rabbits were administered 2×10^9 bacteria of the SEC-positive strain CA-MRSA USA400 MW2, intrabronchially. Although other SAg genes are present in this strain, it is important to note that SEC is secreted at more than 2500-fold higher concentrations than other SAgs in MW2 (see Materials and methods), suggesting that among the SAgs one might expect SEC to have the most significant hyperinflammatory effect. Treatment consisted of i.v. injection of 500 μg Vβ L3 or PBS daily. Temperatures were measured daily, as was survival. Three of the four rabbits that were given MW2 followed by the control PBS died over the 4 days (Fig. 7B). The control rabbits had an increase in body temperature that peaked on the second day (Fig. 7A). All four of the rabbits that received the Vβ L3 survived, and their temperatures remained normal (Fig. 7A and B). Thus, Vβ L3 was able to neutralize the SEC secreted by MW2 and survival of the treated rabbits was significant with $P < 0.05$.

Neutralization of SEC secreted by MW2 in an infective endocarditis rabbit model

There has been evidence that TSST-1 is involved in infective endocarditis in a rabbit model (Pragman *et al*., 2004), and its prevalence in *S.aureus* isolates from human endocarditis suggests that it is involved in the human disease (Nienaber *et al*., 2011). Having already shown that L3 could neutralize the toxin alone, and also prevent lethality caused by the MW2 strain in the pneumonia model, we explored the ability

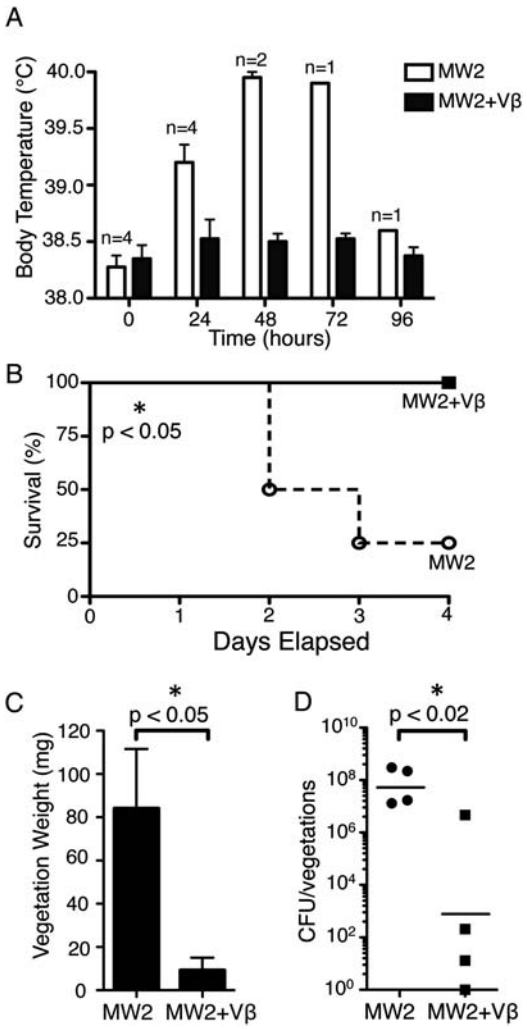

Fig. 7. *In vivo* models testing Vβ L3 neutralization of MW2 SEC secreting bacteria. (**A**) and (**B**) Necrotizing pneumonia model. Rabbits were intrabronchially administered 2×10^9 bacteria of the CA-MRSA USA400 strain MW2, which secretes SEC. Treatment consisted of either an i.v. of 500 μg Vβ L3 or PBS daily. (**A**) Temperatures in rabbits administered Vβ remained low while rabbits that received MW2 only had an increase in temperature. The error bars represent SEM. (**B**) One of four rabbits survived when injected with MW2 alone. The Vβ L3 is able to neutralize the toxin yielding survival of 4/4 rabbits. *P* value of (**B**) ($P < 0.05$) determined by log-rank (Mantel–Cox) test ($n = 4$ per group). (**C**) and (**D**) Endocarditis model. Vegetations were isolated and weighed either at death or on Day 4. PBS-treated rabbits ($n = 4$) developed multiple large vegetations with a mean weight of 84 mg (**C**) and 6.18×10^7 CFU/vegetations (**D**). The Vβ L3-treated rabbits ($n = 4$) had either no or small vegetations with a mean weight of 9 mg (**C**) and 340 CFU/vegetations (**D**). Both the average weight of the vegetation and the CFU/vegetations were statistically significant with *P* values <0.05. *P* values determined by two-tailed unpaired *t*-test ($n = 4$ per group). The error bars represent SEM.

of L3 to neutralize SEC in an infective endocarditis rabbit model, with the MW2 strain (Schlievert *et al.*, 1998). In this model, catheters are inserted into anesthetized rabbits to the aortic valves where the catheter damages the valves for 2 h prior to removal. Infective endocarditis was modeled by injecting $\sim 10^8$ SEC-secreting bacteria USA400 strain MW2 into the marginal ear vein, allowing for formation of vegetations at the valve sites for up to 4 days, similar to that observed in infective endocarditis. Rabbits were administered either the control PBS (pH 7.4) or 100 μg of Vβ L3 twice daily and examined for survival four times daily and for vegetations upon death or on Day 4 upon euthanasia.

Two of the four rabbits infected only with MW2, but without L3 treatment, died before the fourth day (one within 24 h and the second at 48 h). The rabbit that died at 24 h developed a single vegetation of 17 mg with 1.3×10^7 colony-forming units (CFUs)/vegetations (Fig. 7C and Supplementary Fig. S3C). The relatively rapid death of this rabbit likely accounts for the smaller vegetation size compared with the other rabbits. The other rabbits infected only with MW2, but without L3 treatment, developed multiple large vegetations (Fig. 7C and Supplementary Fig. S3A–B and S3D) with an average weight of 84 mg and 6.2×10^7 CFU/vegetations (Fig. 7C and D).

One of the four rabbits, which was administered Vβ L3, died at 72 h, and the other three were euthanized at Day 4 (as required by IACUC protocol). In contrast to the control (PBS) rabbits, all four of the Vβ L3-treated rabbits had either no or only small vegetations (Supplementary Fig. S3E–H). In addition, the average vegetation weight of organisms derived from the Vβ L3-treated rabbits was 9.2 mg and 340 CFU/vegetations (Fig. 7C and D). Although significant (*P* values of 0.038 and 0.013, respectively, for weight and CFU/vegetations) these data were skewed somewhat because the one Vβ-treated rabbit that died at 72 h had 4.7×10^6 CFU when the aortic valve surface was scraped and analyzed (Fig. 7D), but this was still below that of any of the control rabbits.

Discussion

We show here that a small protein domain (Vβ) of the extracellular receptor for SEC could be engineered for high affinity against SEC, and that the engineered protein (L3) cross-reacted, unexpectedly but fortuitously, with the related toxin SEB. Consistent with these binding properties, L3 was able to neutralize both SEC and SEB in T cell activation assays *in vitro*. L3 was also able to not only protect rabbits from the lethality associated with exposure to the toxin SEC itself, but it also protected rabbits from the lethality caused by a strain of MRSA (MW2) that secretes SEC. Successful treatment of rabbits infected in the lung with the MW2 strain, in the necrotizing pneumonia model, is likely due to the specific anti-inflammatory properties of the neutralizing agent. Treatment of MW2 in the infective endocarditis model also yielded beneficial results, with a reduction in vegetation size, although the mechanism of action of the neutralizing agent in this model is less clear and remains to be determined. Nevertheless, the results suggest an important role for the SAg in this disease, and they provide further evidence that these small, high-affinity protein domains represent a therapeutic strategy that could show efficacy, even in cases where antibiotics have limited or delayed impact.

SAg genes have been identified in the majority of MRSA strains from various clinical diseases (e.g. Campbell *et al.*, 2008; Lalani *et al.*, 2008; Xiong *et al.*, 2009; DeVries *et al.*, 2011; Robert *et al.*, 2011; Sharma-Kuinkel *et al.*, 2011) and they have recently been found to be carried by VRSA strains (Kos *et al.*, 2012). In addition to their emergence in antibiotic-resistant strains, SAgs secreted by *S.aureus* and group A streptococci have been shown to contribute to multiple illnesses including TSS, necrotizing pneumonia, purpura fulminans and extreme pyrexia syndrome (Luppi *et al.*, 1998; Bachert *et al.*, 2007; Strandberg *et al.*, 2010).

Clinical and epidemiological features also implicate SAgs in diseases such as atopic dermatitis and Kawasaki syndrome (Leung *et al.*, 2002; Schlievert *et al.*, 2008; Macias *et al.*, 2011). A recent study showed that the SAg TSST-1 gene was among the few genes significantly associated with isolates derived from endocarditis patients (Nienaber *et al.*, 2011). Despite advances in acute care and antibiotics, mortality rates due to staphylococcal infections remain high. As neither the treatment of symptoms nor antibiotics are capable of removing SAgs already secreted by the bacteria and present within tissues of the host, the relatively small (~14 kDa) agents described here may be able to penetrate affected tissues and reduce the hyperinflammatory effects of SAgs.

Our previous studies with a high-affinity neutralizing agent against SEB showed that the Vβ G5-8 could be used to treat pulmonary disease (Strandberg *et al.*, 2010), thereby implicating the SAg in lung disease. It was reasonable to assume that some of the pulmonary effects of SAgs were due to the massive inflammation that the toxins induce, and thus treatment with an agent that acts early in the cascade mechanism could impact the disease. In the infective endocarditis model, the direct role of SAgs may be less clear, but the observation that the Vβ neutralizing agent showed significant effects implies that the process of endocarditis caused by *S.aureus* involves the functional effects, or dysregulation, of T cells at the site of the damaged valves.

Based on our previous engineering of the high-affinity Vβ G5-8 against SEB (Buonpane *et al.*, 2007), we used G5-8 in several rabbit models of SEB-mediated diseases, including TSS (Buonpane *et al.*, 2007), necrotizing pneumonia (Strandberg *et al.*, 2010) and atopic dermatitis (John *et al.*, 2009) exacerbated by SEB. However, the Vβ regions previously engineered against SEB did not cross-react with high affinity against the structurally related SAg SEC, despite the two SAgs sharing 65% homology (Bohach *et al.*, 1990; McCormick *et al.*, 2001; Wang *et al.*, 2010). As SEC is important in disease, and often expressed by the USA400 strains of MRSA, here we elected to further engineer a high-affinity Vβ against SEC, called L2CM (Kieke *et al.*, 2001), to improve its affinity and its neutralizing potential. L2CM was originally engineered by random mutagenesis, and with improved strategies for site-directed mutagenesis we focused on libraries within the Vβ loops nearest to the SEC binding interface, HV4 and CDR2. A strong preference for several HV4 residues was observed in the improved Vβ mutants, including a tryptophan at position 72. It is reasonable to suggest that part of the improved affinity for SEC and its higher affinity for SEB is related to Trp72 proximity to the SAg residue Tyr90, which is found in both SEB and SEC3 (Fig. 1C), perhaps through additional buried hydrophobicity or stacking.

While Trp72 and the HV4 mutations may account for some of the additional binding energy for both SEC and SEB, it is possible that both the CDR1 and CDR2 mutations in L3 may also act synergistically. For example, the additional residue in CDR1 has been shown to position the Tyr28 to contact Asn60 in the G5-8/SEB structure, and Asn60 is shared between SEB and SEC (Fig. 1D). Furthermore, our recent studies have suggested that the Arg53 mutation of the SEB-reactive G5-8 prevents high-affinity binding to SEC because the unique tyrosine of SEC at position 26 occupies the pocket that Arg53 is inserted into in SEB (Wang *et al.*, 2010; Bonsor *et al.*, 2011). In contrast, our previous extensive structural and binding analyses of Val52 and Asn54 in L2CM have shown that these mutations act through multiple mechanisms, pre-configuring the Vβ surface for binding and also increasing the contacts with SEC (Cho *et al.*, 2005). Furthermore, the retention of the wild-type Gly53 in L3 likely allows the Val52 and Asn54 residues to engage SEC, yet still interact effectively with SEB. It is possible that these CDR1 and CDR2 interactions were not adequate to raise the affinity above a threshold binding needed for flow cytometry with 10 nM SEB, but that combined with the HV4 mutations they yielded the final nanomolar affinity for SEB. Regardless of the exact structural details, which will require crystallization of the complexes, the results with L3 show that it is possible to engineer a protein domain that can bind with high affinity to two different ligands by manipulating different regions of the interface.

In summary, we show that it is possible to use an engineered, high-affinity neutralizing agent against SEC to further demonstrate the importance of SEC in rabbit models of disease. Accordingly, the neutralizing protein L3 reduced the lethality and severity in two disease animal models, necrotizing pneumonia and infective endocarditis caused by SEC-positive CA-MRSA USA400 strain MW2. Quantitative analysis of bacterial burden, both by weighing scraped tissue and colony counts revealed a significantly lower total weight of vegetations as well as fewer CFUs/vegetations in the L3-treated rabbits compared with the control (PBS)-treated rabbits in the infective endocarditis model (Fig. 7C and D). The inhibition of vegetation development further supports the notion that SAgs play an important role in the etiology of infective endocarditis. Although there are no doubt other factors that are important in these disease etiologies, our evidence suggests that *S.aureus* SAgs may provide one target for treatment. The high-affinity and *in vitro* effectiveness of the Vβ L3 for both SEC and SEB indicates a potential use as a therapeutic against bacterial strains that may secrete either or both SAgs. While antibiotics constitute the major approach to treatment of infective endocarditis (Sacar *et al.*, 2010) and necrotizing pneumonia (Shilo and Quach, 2011), the mortality rates in these staphylococcal diseases, especially MRSA, remain high (Fowler *et al.*, 2005) and thus it is important to identify novel strategies to intervene.

Supplementary data

Supplementary data are available at *PEDS* online.

Acknowledgements

We thank the staff of University of Illinois Biotechnology Center for assistance in flow sorting and DNA sequencing.

Funding

This work was supported by National Institutes of Health grants (R01-AI064611 to D.M.K.), (R01-AI065690 to E.J.S.), National Institutes of Health under Ruth L. Kirschstein National Research Service Award (F30-HL096352-01 to D.M.M.) and a grant from the National Institutes of Health-supported Great Lakes Regional

Center for Excellence in Biodefense and Emerging Diseases (U54 AI57153 to P.M.S. and D.M.K.).

References

Bachert,C., Gevaert,P., Zhang,N., van Zele,T. and Perez-Novo,C. (2007) *Chem. Immunol. Allergy*, **93**, 214–236.

Boder,E.T. and Wittrup,K.D. (2000) *Methods Enzymol.*, **328**, 430–444.

Bohach,G.A., Fast,D.J., Nelson,R.D. and Schlievert,P.M. (1990) *Crit. Rev. Microbiol.*, **17**, 251–272.

Bonsor,D.A., Postel,S., Pierce,B.G., Wang,N., Zhu,P., Buonpane,R.A., Weng,Z., Kranz,D.M. and Sundberg,E.J. (2011) *J. Mol. Biol.*, **411**, 321–328.

Buonpane,R.A., Churchill,H.R., Moza,B., Sundberg,E.J., Peterson,M.L., Schlievert,P.M. and Kranz,D.M. (2007) *Nat. Med.*, **13**, 725–729.

Campbell,S.J., Deshmukh,H.S., Nelson,C.L., *et al*. (2008) *J. Clin. Microbiol.*, **46**, 678–684.

Cho,S., Swaminathan,C.P., Yang,J., Kerzic,M.C., Guan,R., Kieke,M.C., Kranz,D.M., Mariuzza,R.A. and Sundberg,E.J. (2005) *Structure*, **13**, 1775–1787.

Churchill,H.R., Andersen,P.S., Parke,E.A., Mariuzza,R.A. and Kranz,D.M. (2000) *J. Exp. Med.*, **191**, 835–846.

Derzelle,S., Dilasser,F., Duquenne,M. and Deperrois,V. (2009) *Food Microbiol.*, **26**, 896–904.

DeVries,A.S., Lesher,L., Schlievert,P.M., Rogers,T., Villaume,L.G., Danila,R. and Lynfield,R. (2011) *PLoS One*, **6**, e22997.

Dinges,M.M. and Schlievert,P.M. (2001) *Infect. Immun.*, **69**, 7169–7172.

Fey,P.D., Said-Salim,B., Rupp,M.E., Hinrichs,S.H., Boxrud,D.J., Davis,C.C., Kreiswirth,B.N. and Schlievert,P.M. (2003) *Antimicrob. Agents Chemother.*, **47**, 196–203.

Fowler,V.G., Jr., Miro,J.M., Hoen,B., *et al*. (2005) *J. Am. Med. Assoc.*, **293**, 3012–3021.

Fraser,J.D. and Proft,T. (2008) *Immunol. Rev.*, **225**, 226–243.

Holler,P.D. and Kranz,D.M. (2003) *Immunity*, **18**, 255–264.

John,C.C., Niermann,M., Sharon,B., Peterson,M.L., Kranz,D.M. and Schlievert,P.M. (2009) *Clin. Infect. Dis.*, **49**, 1893–1896.

Kieke,M.C., Sundberg,E., Shusta,E.V., Mariuzza,R.A., Wittrup,K.D. and Kranz,D.M. (2001) *J. Mol. Biol.*, **307**, 1305–1315.

Kos,V.N., Desjardins,C.A., Griggs,A., *et al*. (2012) *MBio*, **3**(3):e00112-12. doi:10.1128/mBio.00112-12.

Lalani,T., Federspiel,J.J., Boucher,H.W., *et al*. (2008) *J. Clin. Microbiol.*, **46**, 2890–2896.

Leung,D.Y., Meissner,H.C., Shulman,S.T., *et al*. (2002) *J. Pediatr.*, **140**, 742–746.

Li,H., Llera,A., Malchiodi,E.L. and Mariuzza,R.A. (1999) *Annu. Rev. Immunol.*, **17**, 435–466.

Lowy,F.D. (1998) *N. Engl. J. Med.*, **339**, 520–532.

Luppi,P., Rudert,W.A., Zanone,M.M., *et al*. (1998) *Circulation*, **98**, 777–785.

Macias,E.S., Pereira,F.A., Rietkerk,W. and Safai,B. (2011) *J. Am. Acad. Dermatol.*, **64**, 455–472; quiz 473–454.

Marrack,P. and Kappler,J. (1990) *Science*, **248**, 705–711.

McCormick,J.K., Yarwood,J.M. and Schlievert,P.M. (2001) *Annu. Rev. Microbiol.*, **55**, 77–104.

Mertz,P.M., Cardenas,T.C., Snyder,R.V., Kinney,M.A., Davis,S.C. and Plano,L.R. (2007) *Arch. Dermatol.*, **143**, 1259–1263.

Moza,B., Buonpane,R.A., Zhu,P., Herfst,C.A., Rahman,A.K., McCormick,J.K., Kranz,D.M. and Sundberg,E.J. (2006) *Proc. Natl Acad. Sci. USA*, **103**, 9867–9872.

Nienaber,J.J., Sharma Kuinkel,B.K., Clarke-Pearson,M., *et al*. (2011) *J. Infect. Dis.*, **204**, 704–713.

Papageorgiou,A.C. and Acharya,K.R. (1997) *Structure*, **5**, 991–996.

Parsonnet,J., Gillis,Z.A., Richter,A.G. and Pier,G.B. (1987) *Infect. Immun.*, **55**, 1070–1076.

Pragman,A.A., Yarwood,J.M., Tripp,T.J. and Schlievert,P.M. (2004) *J. Bacteriol.*, **186**, 2430–2438.

Resch,A., Wilke,M. and Fink,C. (2009) *Eur. J. Health Econ.*, **10**, 287–297.

Robert,J., Tristan,A., Cavalie,L., Decousser,J.W., Bes,M., Etienne,J. and Laurent,F. (2011) *Antimicrob. Agents Chemother.*, **55**, 1734–1739.

Sacar,M., Sacar,S., Cevahir,N., *et al*. (2010) *Tex. Heart Inst. J.*, **37**, 400–404.

Schlievert,P.M. (1982) *Infect. Immun.*, **36**, 123–128.

Schlievert,P.M., Case,L.C., Nemeth,K.A., *et al*. (2007) *Biochemistry*, **46**, 14349–14358.

Schlievert,P.M., Case,L.C., Strandberg,K.L., Abrams,B.B. and Leung,D.Y. (2008) *Clin. Infect. Dis.*, **46**, 1562–1567.

Schlievert,P.M., Gahr,P.J., Assimacopoulos,A.P., Dinges,M.M., Stoehr,J.A., Harmala,J.W., Hirt,H. and Dunny,G.M. (1998) *Infect. Immun.*, **66**, 218–223.

Sharma-Kuinkel,B.K., Ahn,S.H., Rude,T.H., *et al*. (2011) *J. Clin. Microbiol.*, **50**, 848–856.

Shilo,N. and Quach,C. (2011) *Paediatr. Respir. Rev.*, **12**, 182–189.

Strandberg,K.L., Rotschafer,J.H., Vetter,S.M., Buonpane,R.A., Kranz,D.M. and Schlievert,P.M. (2010) *J. Infect. Dis.*, **202**, 1690–1697.

Wang,N., Mattis,D.M., Sundberg,E.J., Schlievert,P.M. and Kranz,D.M. (2010) *Clin. Vaccine Immunol.*, **17**, 1781–1789.

Xiong,Y.Q., Fowler,V.G., Yeaman,M.R., Perdreau-Remington,F., Kreiswirth,B.N. and Bayer,A.S. (2009) *J. Infect. Dis.*, **199**, 201–208.